Computers Math. Applic. Vol. 24, No. 12, pp. 99–120, 1992
Printed in Great Britain

0097-4943/92 $5.00 + 0.00
Pergamon Press Ltd

IMPROVED ACCURACY OF MULTIQUADRIC INTERPOLATION USING VARIABLE SHAPE PARAMETERS

E. J. KANSA AND R. E. CARLSON
Lawrence Livermore National Laboratory
P.O. Box 808, Livermore, CA 94550, U.S.A.

Abstract—Given N scattered data points, we examined the problem of finding N variable Multiquadric (MQ) shape-parameters, or R^2 values. Because the problem of finding the optimal R^2 values is a nonlinear one, we optimized these parameters numerically by minimizing the root-mean-square (RMS) errors. The resulting R^2 values varied over many orders of magnitude. We have tested this approach on a number of univariate and bivariate (Franke's) problems, and found that the RMS error reduction was substantial.

1. INTRODUCTION

We study the problem of multi-variate scattered data interpolation which can be defined as follows: given a set of points, $\underline{x}_i \in \mathbf{R}^d, \{(x_i^1, x_i^2, \ldots, x_i^d), i = 1, 2, \ldots, N\}$, and a set of N real numbers, $\{f(\underline{x}_i), i = 1, 2, \ldots, N\}$, then a function $F(\underline{x})$ which satisfies

$$F(\underline{x}_i) = f_i, \quad i = 1, 2, \ldots, N \tag{1}$$

is said to be an interpolant of f.

We are interested in studying radial basis function methods for the scattered data interpolation problem which have the form

$$F(\underline{x}) = \sum_{j=1}^{N} \lambda_j \, \Phi(\|\underline{x} - \underline{x}_j\|), \tag{2}$$

where λ_j, $j = 1, 2, \ldots, N$ are found by solving a set of linear equations,

$$F(\underline{x}_i) = \sum_{j=1}^{N} \lambda_j \, \Phi(\|\underline{x}_i - \underline{x}_j\|), \tag{3}$$

where $\|\cdot\|$ means the Euclidean norm, and $\Phi(\|\underline{x} - \underline{x}_j\|)$ are the basis functions.

One of the most important radial basis function methods is Multiquadric (MQ) developed by Hardy [1]. The MQ interpolant has the form

$$\Phi(\|\underline{x} - \underline{x}_j\|) = [\,\|\underline{x} - \underline{x}_j\|^2 + R^2\,]^{1/2}, \quad j = 1, 2, \ldots, N, \tag{4}$$

where R^2 is an input shape-parameter which is independent of j. We will denote this form of Multiquadrics as constant (R^2) multiquadric (CMQ).

An important unsolved problem is finding a method for computing the optimal value of R^2 for CMQ. Carlson and Foley [2] have shown that the optimal value of R^2 depends on the function values, $\{f_i\}$, and is almost independent of the set of $\{\underline{x}_i\}$. They developed an empirical relation for computing R^2, and no theory exists for computing the optimal R^2 for CMQ.

Work performed under the auspices of the U. S. Department of Energy by the Lawrence Livermore National Laboratory under contract number W-7405-ENG-48.

Tarwater [3] showed, that the root-mean-squared (RMS) errors of the interpolants decrease with increasing R^2 up to a value of R^2_{optimal}. Beyond the optimal value of R^2, the RMS errors often increase dramatically, particularly as the associated linear system of equations becomes ill-conditioned.

Narcowich and Ward [4] obtained estimates on $\sqrt{1+\|x\|^2}$ rather than $\sqrt{R^2+\|x\|^2}$ for the norms of inverses and condition numbers associated with the coefficient matrices for three types of radial basis functions including CMQ. If we let q be one-half of the minimum separation distance between data points and $D = \max_{i\neq j} |\underline{x}_i - \underline{x}_j|$, then the condition number, K, for the CMQ bivariate case tends to diverge as (see [4])

$$K \to 12 \exp\left(\frac{6}{q^2}\right) D^3 \frac{\sqrt{1+D^2}}{q^5}, \qquad \text{for } q \to 0+. \tag{5}$$

K is bounded from above by

$$K \to 6 \frac{\sqrt{1+D^2}}{q}, \qquad q \to \infty. \tag{6}$$

The effect of increasing R^2 is to decrease the minimum separation distance. In many cases, 1 (as used in [4]) might already be too large. Similar conclusions exist for 3 dimensions.

Until now, all discussion has been with a constant shape parameter, R^2. Although Hardy [5] had experimented with allowing R^2 also to depend on j, he abandoned this approach in favor of the simpler CMQ. Kansa [6–8] used a variable R^2 form of MQ (VMQ) with a basis function of the form

$$\Phi(\|\underline{x} - \underline{x}_j\|) = [\,\|\underline{x} - \underline{x}_j\|^2 + R_j^2\,]^{1/2}, \tag{7}$$

where R_j^2 has the empirical form for strictly monotone f

$$R_j^2 = R^2_{\min}\left(\frac{R^2_{\max}}{R^2_{\min}}\right)^{\frac{j-1}{N-1}}, \quad j = 1,2,\ldots,N, \tag{8}$$

where $R^2_{\min}$ and $R^2_{\max}$ are two input parameters. If $R^2_{\min}$ and $R^2_{\max}$ vary by several orders of magnitude, and if the underlying function varies rapidly, then very accurate definite integrals, interpolants, and partial derivatives can be obtained. However, because the R_j^2's are the same for a given column, very large values of R_j^2 still gives ill-conditioning, although the growth rate of the condition number is considerably less than for CMQ.

Although very accurate results were obtained, a drawback is that the coefficient matrix is no longer symmetric. This lack of symmetry is, as will be shown, a small price to pay for the benefits of vastly improved accuracy. In this paper, we show that VMQ is capable of handling very disparate values of R^2 while keeping reasonable bounds on the condition number. However, in order to obtain very accurate interpolants, partial derivatives and definite integrals, good conditioning is a necessary, but not a sufficient condition. At present there is no theory for predicting either the optimal R^2 for the CMQ scheme, or the set, $\{R_j^2\}$ for the VMQ scheme. By examining the global *minimum* of the RMS errors between families of test functions and their VMQ interpolants, it may be possible to develop empirical relations for the $\{R_j^2\}$ for such families. Such an empirical relation would be very useful until a theory for the VMQ scheme is developed.

In our numerical experiments, we considered a set, $\mathbf{X}$, of N data locations in $\mathbf{R}^d$ denoted by $\mathbf{X} = \{\underline{x}_i, i = 1,2,\ldots,N\}$ with $\underline{x}_i = \{x_i^1, x_i^2, \ldots, x_i^d\}$. In this paper, we will limit ourselves to $d = 1$ or 2. Let $\mathbf{U} = \{\underline{u}_i : i = 1,2,\ldots,M\}$ with $\underline{u}_i = \{u_i^1, u_i^2, \ldots, u_i^d\}$ as the set of evaluation points ($M > N$) which is used to compute the RMS error. For the univariate problems we set $N = 7$ and $\mathbf{U}$ is the uniform mesh of 101 points on [0,1]. For bivariate problems, we used the Franke [9] 25 data point set and $\mathbf{U}$ is the uniform 33×33 grid defined over the unit square.

Our goal was to find the set of N shape parameters, $\{R_j^2\}$, which minimized the RMS error over the points in $\mathbf{U}$, i.e.,

$$Z = \sum_{m=1}^{M} \| f^{\text{exact}}(\underline{u}_m) - \Phi^{\text{MQ}}(\underline{u}_m) \|^2, \tag{9}$$

where

$$\Phi^{\mathrm{MQ}}(\underline{u}_m) = \sum_{j=1}^{N} \lambda_j [\|\underline{u}_m - \underline{x}_j\|^2 + R_j^2]^{1/2}. \tag{10}$$

Two approaches were used to find the optimal set of shape parameters. In the first approach, we solved a nonlinear system of normal equations:

$$\frac{\partial Z}{\partial R_k^2} = 0, \quad \text{for each } k = 1, 2, \ldots, N.$$

The equations were solved using SNSQE from the SLATEC library. In some instances, we have perturbed the distribution of the R_j^2 values in an attempt to find a smaller minimum. The second approach minimizes the sum of squares over the points in **U**. This minimum was computed using SNLSE, also from the SLATEC library. Several different initial guesses were tried using constant R^2 values.

As stated previously, there does not yet exist a theory for choosing an optimal constant R^2, let alone for a variable R^2 distribution. It is our hope that our empirical results can lead to a theory. In the interim, we show that a VMQ scheme can be very effective in solving practical problems.

2. UNIVARIATE RESULTS

In both the univariate and bivariate test function evaluations, we used double precision arithmetic on the CRAY computer. Our univariate studies considered several test functions, with a total number of seven input data points on [0,1].

The univariate test functions were:

(a) sinusodal function, **SIN**, $f(x) = (1/2)\{1 + \sin 6x\}$;
(b) logarithmic function, **LOG**, $f(x) = \log_e(x + 1.2 \times 10^{-7})$;
(c) exponential function, **XP**, $f(x) = \exp(5x)$;
(d) fractional power expressions, **FRAC**, $f(x) = 0.7(x + 1/10)^{0.7} - 0.35(x + 1/11)^{-0.15}$;
(e) step-function approximation, **STEP**, $f(x) = (1/2)[1 + 2/\pi \arctan\{120(x - 1/2)\}]$;
(f) delta-function approximation, **DELT**, $f(x) = 120/[1 + v^2]$, $v = 120 \cdot (x - 1/2)$;
(g) derivative of the delta-function approximation, **DDLT**, $f(x) = -28{,}880 \cdot v/[\{1 + v^2\}^2]$, $v = 120(x - 1/2)$;

In order to find the optimal-constant R^2 parameter for these univariate functions, we calculated the RMS errors using many different values of R^2 using the CMQ scheme. The value of R^2 which yields the minimum RMS error is defined as R^2_{opt}. Using R^2_{opt} as a starting guess, we used SNSQE to compute a set $\{R_j^2\}$. Plots of these results are provided in Appendix A.

Table 1 is a comparison of the RMS errors and estimated condition number between CMQ and VMQ algorithms. The optimal values for R_j^2 were computed using SNSQE.

Table 1. RMS errors and condition number of the MQ coefficient matrix for the univariate test functions.

Function	Optimal CMQ		Optimal VMQ	
	Condition No.	RMS Error	Condition No.	RMS Error
SIN	2.8×10^5	1.1×10^{-3}	9.6×10^6	1.0×10^{-4}
LOG	5.7×10^3	3.9×10^{-2}	1.3×10^3	2.0×10^{-3}
XP	1.0×10^7	5.0×10^{-3}	1.2×10^6	1.3×10^{-3}
FRAC	1.0×10^7	1.4×10^{-3}	1.0×10^7	7.8×10^{-5}
STEP	4.4×10^2	6.0×10^{-2}	1.1×10^6	1.2×10^{-3}
DELT	4.3×10^3	5.4×10^{-2}	9.2×10^6	1.1×10^{-3}
DDLT	2.5×10^3	4.4×10^{-2}	7.5×10^5	9.3×10^{-3}

Table 2. Data locations of the univariate test functions on [0,1].

Function	x_1	x_2	x_3	x_4	x_5	x_6	x_7
SIN	−0.001	0.22	0.34	0.50	0.66	0.78	1.001
LOG	0.0	0.035	0.060	0.15	0.30	0.60	1.00
XP	0.0	0.40	0.57	0.79	0.82	0.95	1.00
FRAC	0.001	0.22	0.34	0.50	0.66	0.75	1.001
STEP	−0.001	0.483	0.49236	0.50	0.50764	0.5170	1.0001
DELT	−0.001	0.483	0.49236	0.50	0.50764	0.5170	1.0001
DDLT	0.0001	0.483	0.49236	0.50	0.50764	0.5170	1.0001

Of the seven data points two were located at or near the endpoints, and the other five points were adjusted in order to capture the essence of the shape of each curve by a piecewise linear fit. The interpolation points for each curve are given in Table 2.

In Table 3, we list the optimal-constant R^2 values we found which minimizes the RMS errors for the univariate test functions at the locations given in Table 2.

Table 3. Optimal-constant R^2 values of the univariate test functions.

Function	Optimal-Constant R^2
SIN	0.32
LOG	5.5×10^{-7}
XP	85.0
FRAC	75.0
STEP	9.0×10^{-7}
DELT	5.5×10^{-5}
DDLT	2.0×10^{-5}

Table 4 is the list of the optimized-variable R^2 values corresponding to locations $x_1, x_2, \ldots, x_7$ for each of the univariate test functions.

Table 4. Optimized R^2 values for the univariate test functions.

Function	R_1^2	R_2^2	R_3^2	R_4^2
SIN	0.29047	0.29419	523.452	0.54835
LOG	4.857×10^{-9}	4.658×10^{-7}	6.161×10^{-4}	5.219×10^{-2}
XP	4.087×10^{0}	2.9209×10^{3}	6.287×10^{3}	6.393×10^{6}
FRAC	4.818×10^{-3}	3.445×10^{3}	1.692×10^{3}	8.759×10^{-1}
STEP	3.421×10^{2}	1.4666×10^{-3}	4.304×10^{-5}	6.955×10^{-4}
DELT	6.496×10^{4}	9.773×10^{-5}	2.036×10^{-5}	2.091×10^{-5}
DDLT	4.818×10^{3}	3.983×10^{-5}	5.804×10^{-21}	2.863×10^{-5}

Function	R_5^2	R_6^2	R_7^2
SIN	0.34988	0.30364	0.25335
LOG	1.860×10^{-2}	1.872×10^{-1}	2.055×10^{-7}
XP	1.543×10^{8}	1.869×10^{9}	4.766×10^{10}
FRAC	7.177×10^{2}	5.528×10^{2}	8.747×10^{3}
STEP	4.825×10^{-5}	1.257×10^{-3}	4.648×10^{-2}
DELT	3.038×10^{-5}	1.2116×10^{-4}	2.283×10^{2}
DDLT	9.093×10^{-19}	3.985×10^{-5}	1.129×10^{5}

Discussion of Univariate Results.

We see that the results for constant R^2 are quite good for the sinusoidal and fractional power functions, fair for the exponential and logarithm test functions, and poor for the step, delta and derivative of the delta function approximations. The latter three approximations vary rapidly over a small neighborhood of $x = 1/2$, but are nearly constant elsewhere. The very small constant-optimal R^2 values for these three functions are nearly piecewise linear fits. However, the optimized variable R_j^2's range over several orders of magnitude, and are somewhat similar in their variation for the step function approximation, and its first and second derivatives. The variables R_j^2's do very well in capturing the rapid variations of the functions near $x = 1/2$.

The logarithm function increases very rapidly near $x = 0$, but gradually tends toward a smooth asymptote. The action of the variable R_j^2's is basically to smooth the VMQ interpolant giving a more visually pleasing result. We also conclude from our numerical experiments that a well-conditioned coefficient matrix is a necessary, but not a sufficient condition for a good CMQ or VMQ approximation.

We can interpret the role of the variable shape parameter in the MQ expansion as a superposition of basis functions ranging from the shape of a rounded cone for very small R^2, a bowl for intermediate values of R^2, and a plate for very large values of R^2. The optimization procedure selects the best finite set of *shape basis functions* to fit the test function. However, the expression *optimal set of shape parameters* should be taken with the caveat that we have probably found a local minimum. We are not guaranteed by our calculus-based numerical optimization procedures that we have found the global minimum. We explore this point in the next section.

3. BIVARIATE FUNCTIONS

Franke [9] used a collection of six bivariate functions and three scattered data sets to compare the performance of a number of scattered data interpolation schemes. The method which he found to perform the best was Hardy's CMQ, where R^2 was computed as a function of the number of data points and the location of the interpolation points in the plane. Carlson and Foley [2] showed that the optimal R^2 is nearly independent of N (the number of data points), and, when mapped onto a unit square, R^2 is nearly independent of the data locations as well. The bivariate set of data points which we have studied is Franke's 25 point data set shown in Figure 1.

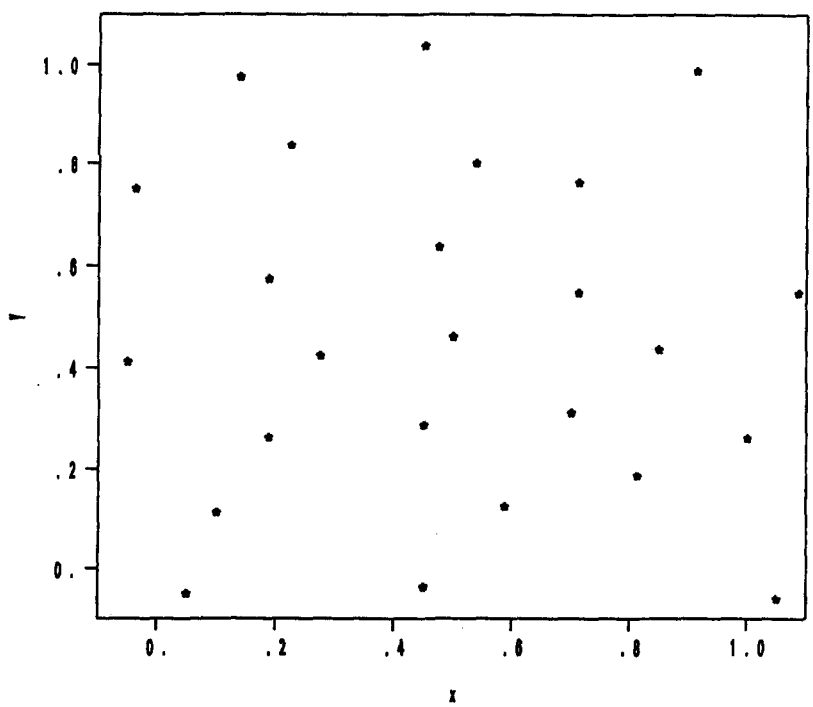

Figure 1. The bivariate 25 point data set of Franke.

As with Carlson and Foley [2], we used Nielson's [10] affine invariant metric which maps the data set onto an ellipse. We observed that the optimal R^2 was shifted to larger values in general, and the condition numbers of the linear system of equations was about an order of magnitude lower than when using the Euclidean metric.

The question we wish to answer in our optimization numerical experiments of the bivariate Franke functions are:

- Does the metric influence RMS errors?
- Does the initial guess affect the RMS errors?
- Does the approach used to minimize the RMS error affect the VMQ solution?

We examined the question of metrics by using the Euclidean metric and Nielson's [10] affine invariant metric (AIM). Later, we shall present the results of numerical experiments involving affine transformations of the data set.

We first examine the results obtained by using AIM. Since the data in AIM are scaled and rotated differently than with the Euclidean metric, the constant-optimal values of R^2 are generally larger than that obtained with the Euclidean metric. We started our optimization procedure using the optimal-constant R^2 values. The AIM scheme was used for both the optimal CMQ as well as the VMQ schemes in this particular study.

In this problem set, we optimized the VMQ scheme for each of the Franke functions by varying each $R_j^2, j = 1, 2, \ldots, 25$ using SNSQE. We summarize our results in the following tables:

Table 5. Estimated condition number, K, and RMS errors using the optimal CMQ-AIM and VMQ-AIM.

Function Number	Optimal CMQ-AIM		VMQ-AIM	
	RMS Error	K	RMS Error	K
1	3.3×10^{-2}	3.03×10^{3}	1.6×10^{-2}	3.22×10^{3}
2	2.4×10^{-2}	2.53×10^{3}	2.3×10^{-3}	2.98×10^{3}
3	4.9×10^{-3}	2.36×10^{7}	3.3×10^{-3}	1.77×10^{6}
4	4.0×10^{-4}	1.04×10^{7}	2.0×10^{-4}	1.01×10^{4}
5	4.2×10^{-3}	3.63×10^{3}	2.1×10^{-3}	2.59×10^{3}
6	1.0×10^{-3}	2.47×10^{8}	9.4×10^{-4}	9.2×10^{10}

We observe VMQ significantly improves the agreement between the interpolant and the exact function in regions in which the exact function has relatively large values in magnitude and an appreciable gradient. This "noise" can be also attributed to the fact that along the line $y = 1$, see Figure 1 (Appendix B), this region is data sparse and both CMQ and RMQ are extrapolating rather than interpolating.

We next performed our minimization experiments using the Euclidean metric, (EM), and the Levenberg-Marquardt scheme using the routine, SNS1E, from the SLATEC library. Rather than starting from the R^2_{opt}, we used three different constant R^2 starting values: $R^2 = 0.001$, 0.1 and 0.9. We summarize our results in the following table of RMS values.

Table 6. Summary of RMS errors using the Euclidean Metric and three different starting constant R^2 values.

FUNCTION NUMBER	$R^2 = 0.001$		$R^2 = 0.1$		$R^2 = 0.9$	
	CMQ-RMS	VMQ-RMS	CMQ-RMS	VMQ-RMS	CMQ-RMS	VMQ-RMS
1	4.1×10^{-2}	1.8×10^{-2}	3.2×10^{-2}	2.4×10^{-2}	7.2×10^{-2}	2.2×10^{-2}
2	2.5×10^{-2}	9.4×10^{-2}	2.3×10^{-2}	8.5×10^{-3}	3.6×10^{-2}	1.6×10^{-2}
3	1.7×10^{-2}	2.7×10^{-3}	9.9×10^{-3}	2.5×10^{-3}	4.6×10^{-3}	4.3×10^{-3}
4	4.8×10^{-3}	3.2×10^{-5}	1.7×10^{-3}	5.2×10^{-5}	3.1×10^{-4}	4.4×10^{-5}
5	1.0×10^{-2}	1.8×10^{-3}	5.3×10^{-3}	1.7×10^{-3}	4.7×10^{-2}	1.4×10^{-3}
6	1.3×10^{-2}	1.2×10^{-3}	7.3×10^{-3}	1.8×10^{-3}	2.2×10^{-3}	1.8×10^{-4}

We tried to minimize the RMS errors in a 25 dimensional space with many different local minima. Consequently, our starting points do influence the location and depth of the local minimum. We note that the affine invariant metric formulation gave lower RMS values than the Euclidean metric formulation for Franke function 1, but the Euclidean metric did better for the remaining functions, however, at different starting values.

We show the Franke 25 point data set in Figure 1, and the exact plot of the functions $f_1, f_2, \ldots, f_6$ in Figures B2, B4, B6, B8, B10, and B12 of Appendix B. The VMQ plots, Figures B8–B13, are the results of the VMQ scheme with the lowest RMS errors taken from Tables 5 and 6. We shall examine the lowest RMS errors VMQ plots of Franke functions f_1, f_2, and f_5 to illustrate the sparsity of data on the Franke 25 data set. For example, f_1 has two peaks and a depression at these approximate locations: (0.15,0.3), (0.7,0.3) and (0.5,0.8). However, we can see from Figure 1 that the data are quite sparse near these extrema. The MQ plot for f_5, see Figure B11, exhibits an oscillatory behavior at the base of the sharp Gaussian along the line, $y = 1.0$. We see from Figure B1 that there is only one datum point along this line at (0.2625,1.0). Except for this point, MQ is extrapolating, rather than interpolating to the line $y = 1.0$.

We note that f_3, f_4, and f_6 appear to perform quite well even in extrapolation with the VMQ scheme.

Hence, we must conclude VMQ can outperform CMQ, but we have not found the global minimum for each one of the Franke functions. This seems to be a deficiency common with calculus-based optimization schemes since one is not guaranteed a global minimum. We will suggest other techniques for finding a global minimum.

Another approach which was successful for VMQ was to transform the input data set by means of a simple affine transformation of the form:

$$\begin{pmatrix} \tilde{x}^1 \\ \tilde{x}^2 \end{pmatrix} = \begin{pmatrix} w_{11} & w_{12} \\ w_{21} & w_{22} \end{pmatrix} \begin{pmatrix} x^1 \\ x^2 \end{pmatrix}. \tag{11}$$

Poggio and Girosi [11] used such an affine transformation by optimizing the elements of the transformation weighting matrix, **W**. They argued that the rows of **W** converge to the eigenvectors of a correlation estimate matrix with the smallest eigenvalues. At convergence, the rows of **W** are close to the eigenvectors of the correlation matrix with the smallest eigenvalues.

In the case where the rows of **W** span a space orthogonal to the principal components of the input data, **W** assigns a metric ellipsoid such that vectors which are far apart in the Euclidean metric are close in the **W** metric if they lie in the hyperplane of the principal components; the nearby vectors in the Euclidean metric are far apart in this metric if they are orthogonal to the principal components.

Similar to Poggio and Girosi [11], we used a constant R^2 starting point, and initialized $w_{11} = w_{22} = 1$ and $w_{12} = w_{21} = 0$. Using SNS1E to minimize the RMS errors, we found a new metric matrix, **W**. For example, for function f_2 with a constant $R^2 = 4.8$, and found the converged values of **W** which gave a transformed data set depicted in Figure 2.

Note that the transformed Franke 25 point data set does appear to form an elongated ellipse as suggested by Poggio and Girosi [11]. Figure 3 shows the plot of f_2 with a constant R^2, and RMS value of 1.0×10^{-3}. The excursion from monotonicity at (0,1) can be attributed to extrapolation.

Using this **W**-metric constant R^2 value as the starting guess, we optimized the set, $\{R_j^2\}$. This time, the RMS errors for f_2 was 3.1×10^{-5}. Figure B5 shows the approximate plot of f_2 which now is visually indistinguishable from the exact plot, Figure B4, Appendix B. (Note the fact that the x-axis in this case, going into the paper, goes from large to small values of x. This is an artifact of the plotting package and is consistent in the rest of the paper.) We have achieved near monotonicity by high accuracy without imposing any constraints on our interpolation scheme by simply transforming the input data set and using variable R^2.

Utreras and Vargas [12] obtained monotonic interpolations of a cliff-function similar to f_2 using the Duchon thin-plate spline by imposing monotonicity constraints.

4. COMMENTS AND CONCLUSIONS

As with most sciences, empirical observations lead to improvements in the theory which in turn suggests more experiments. Although multiquadrics were developed by Hardy [1] over twenty

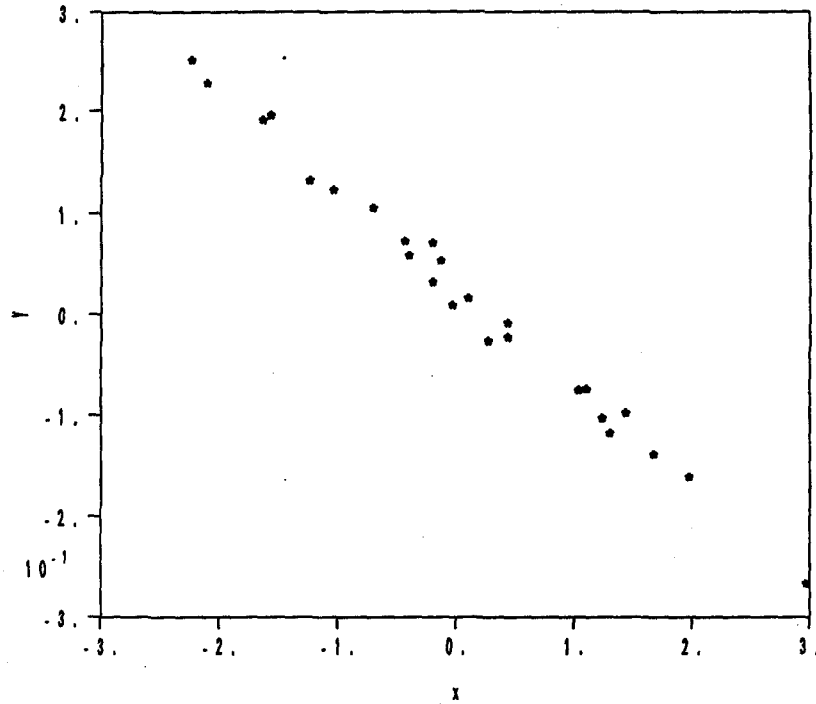

Figure 2. The data locations of the 25 point Franke data set in the W-metric Function 2.

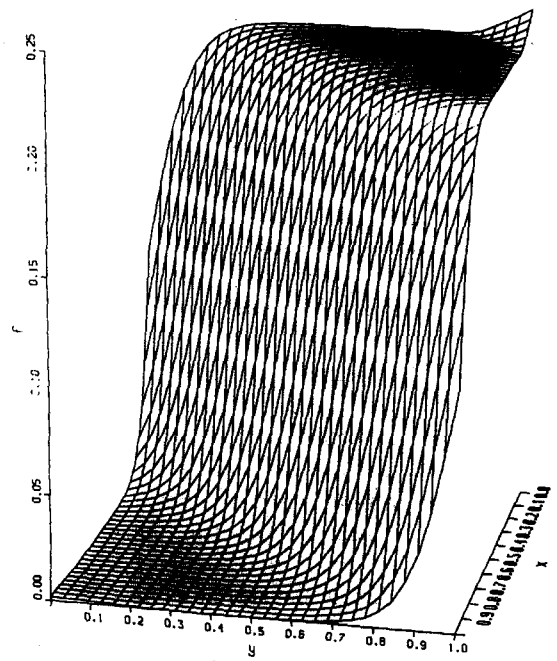

Figure 3. The CMQ plot of Franke's Function 2 using the data locations from the W-metric.

years ago and used successfully in practice in many applications (see Hardy [5]), only recently have theorists begun to develop an understanding why radial basis function methods (including Multiquadrics) work so well. Powell's [13] review of the theory is an excellent summary of the recent developments.

Our empirical results demonstrate that indeed variable shape-parameters can significantly reduce the RMS errors of MQ interpolation as compared to using a constant R^2 approach. As R^2 varies from zero to infinity, the MQ basis function varies from a sharp cone to a flat plate. Our

nonlinear optimization procedure selects a finite, but optimized, number of such basis functions and superimposes them to best match the approximate function with the exact functions.

We used two optimization approaches. One approach focused on the normalized equations, see equation (11), and the other approach focused on the definition of the RMS error. From our results, we can concluded that the R^2_{opt} is not necessarily the best starting point since the calculus based schemes converged to different local minima. Even with the scheme which worked with the definition of the RMS error converged to different minima depending on the initial constant R^2. It appears that our 25 dimensional R^2 parameter space, from the high degree of multi-moduality is not convex.

Goldberg [14] and Otten and van Ginneken [15] have pointed out the deficiencies of the calculus-based optimization schemes in that they do not guarantee global minima, only local minima. We suggest that a more powerful approach such as the genetic algorithm or the annealing algorithm which searches all of the hyper-space and narrows the likely candidates for a global optimization solution set. Then, we can switch to a calculus based algorithm for rapid convergence to the global minimum.

The variable R^2 form of MQ appears to improve the accuracy of the interpolant, especially in the interior regions where the fitted function varies relatively rapidly. However, the variable R^2 method still does not vastly improve the performance of MQ in regions where it must extrapolate rather than interpolate since data locations and function value information constrain MQ.

The variable R^2 scheme did not significantly improve the RMS errors from Franke's function 1 (the best RMS error was 0.016) because a critical lack of data in the region of the "dimple" and along the boundary defined by the line, $y = 1.0$. That region is also responsible for large errors in the approximation to function 5 in which MQ is extrapolating rather than interpolating. No interpolation scheme can be expected to interpolate and extrapolate well in data poor regions.

Another significant result we found in our numerical experiments is that changing to an optimized W-metric can produce dramatic RMS error reduction for Franke's function 2, even for constant R^2 MQ interpolation. Using a variable R^2 scheme in the transformed space, we significantly reduced the RMS errors to 3.1×10^{-5}, yielding a nearly monotonic approximation. We also tried a VMQ scheme which optimized the affine metric on Franke's functions 3 and 5 with RMS errors, 2.2×10^{-3}, and 1.0×10^{-3}, respectively. Unlike function 2, the W matrix for both f_3 and f_5 had diagonal components near 1.0, and off-diagonal components ranging from 10^{-4} to 2×10^{-2}. Further research is required in optimizing the W-metric as well as the $\{R_j^2\}$ which can achieve a global minimum before either a semi-empirical formula can be recommended and before a general theory can be formulated. For interpolation problems in which experimental data is used, we recommend at present to use the CMQ scheme. The estimate of R^2_{opt} obtained from Carlson and Foley [2] is expected to give a very good initial interpolant. Much more research is required in studying the agreement between known test functions and the VMQ interpolant before we would recommend using VMQ on unknown functions represented by a finite amount of data.

The purpose of this report is to inform the community of opportunities in research regarding the open questions of changes in both metrics and shape-parameters to improve significantly an already powerful existing scattered data approximation scheme. We hope that a general theory could be developed.

References

1. R.L. Hardy, Multiquadric equations of topography and other irregular surfaces, *J. Geophys. Res.* **76**, 1905–1915 (1971).
2. R.E. Carlson and T.A. Foley, The parameter R^2 in multiquadric interpolations, *Comp. Math. Applic.* **21** (9), 29–42 (1991).
3. A.E. Tarwater, A parameter study of Hardy's multiquadric method for scattered data interpolation, UCRL-53670, LLNL, (1985).
4. F.J. Narcowich and J.D. Ward, Norms of inverses and condition numbers for matrices associated with scattered data, *J. Approx. Theory* **64**, 69–94 (1991).
5. R.L. Hardy, Theory and applications of the multiquadric-biharmonic method. 20 years of discovery 1968–1988, *Comput. Math. Applic.* **19** (8/9), 163–208 (1990).

6. E.J. Kansa, Multiquadrics—A scattered data approximation scheme with applications to Fluid Dynamics, I. Surface Approximations and Partial Derivative Estimates, *Comput. Math. Applic.* **19** (8/9), 127–145 (1990).
7. E.J. Kansa, Multiquadrics—A scattered data approximation scheme with applications to Fluid Dynamics, II. Solutions to Parabolic Hyperbolic, and Elliptical PDE's, *Comput. Math. Applic.* **19** (8/9), 147–161 (1990).
8. E.J. Kansa, A strictly conservative spatial approximation scheme for the governing engineering and physics equations over irregular relations and inhomogeneously scattered nodes, *Comput. Math. Applic.* (this volume).
9. R. Franke, Scattered data interpolation: Tests of some results, *Math. Comput.* **38**, 181–199 (1982).
10. G.M. Nielson, Coordinate free scattered data interpolations, In *Topics in Multivariate Approximation*, (Edited by L.L. Schumaker, C.C. Hui, and F. Utreras), pp. 175–184, Academic Press, NY, (1987).
11. T. Poggio and F. Girosi, Networks for approximation and learning, In *Proc. IEEE* **78**, 1481–1497 (1990).
12. F. Utreras and M.L. Vargas, Monotone interpolations of scattered data in R^2, *Constr. Approx.* **7**, 49–68 (1991).
13. M.J.D. Powell, The theory of radial basis function approximation in 1990, Tech. Report DAMTP 1990/NA11, University of Cambridge, Cambridge, England.
14. D.E. Goldberg, *Genetic Algorithms in Search, Optimization, and Machine Learning*, Addison-Wesley, Reading, MA, (1989).
15. J.H.J.M. Otten and L.P.P.P. van Ginneken, *The Annealing Algorithm*, Kluwer Academic Publ., Norwell, MA, (1989).

APPENDIX A
PLOTS OF EXACT AND VMQ INTERPOLANTS OF THE UNIVARIATE TEST FUNCTIONS

Table A1. Summary of list of figures for the univariate test functions for optimal CMQ, and VMQ.

Function	Optimal CMQ	VMQ
SIN	Figure A1	Figure A2
LOG	Figure A3	Figure A4
XP	Figure A5	Figure A6
FRAC	Figure A7	Figure A8
STEP	Figure A9	Figure A10
DELT	Figure A11	Figure A12
DDLT	Figure A13	Figure A14

Note the diamonds in the figures are the values of the MQ interpolants, the solid line is the exact function.

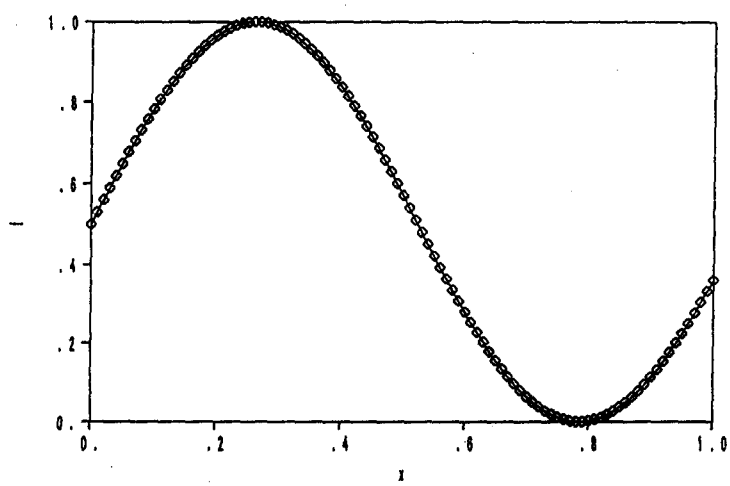

Figure A1. The exact and CMQ plots of the SIN function.

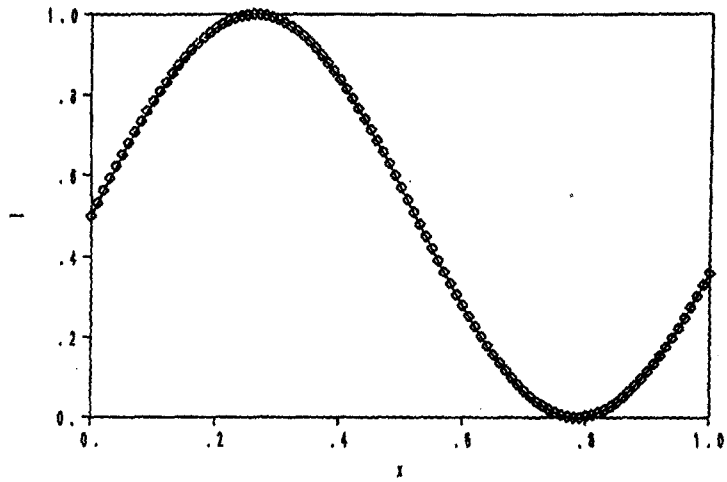

Figure A2. The exact and VMQ plots of the SIN function.

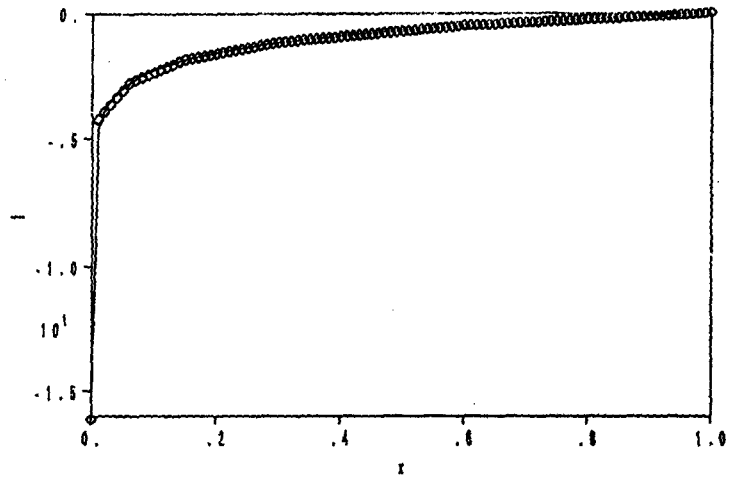

Figure A3. The exact and CMQ plots of the LOG function.

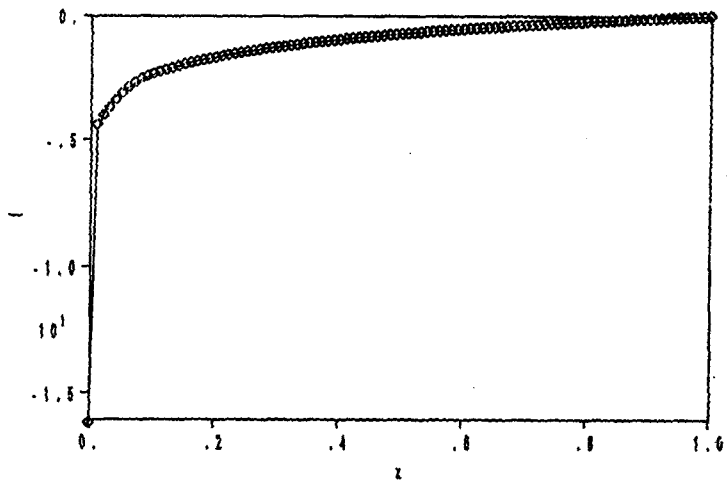

Figure A4. The exact and VMQ plots of the LOG function.

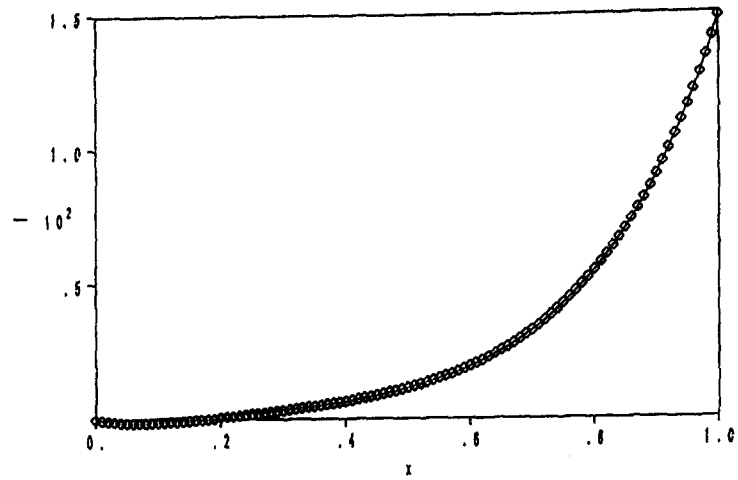

Figure A5. The exact and CMQ plots of the XP function.

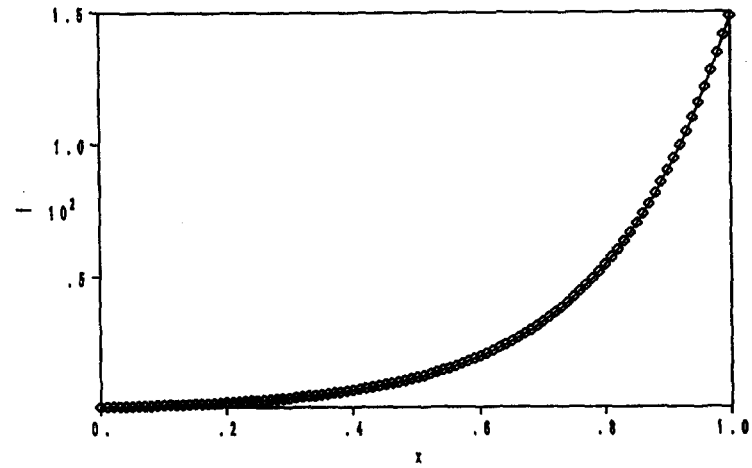

Figure A6. The exact and VMQ plots of the XP function.

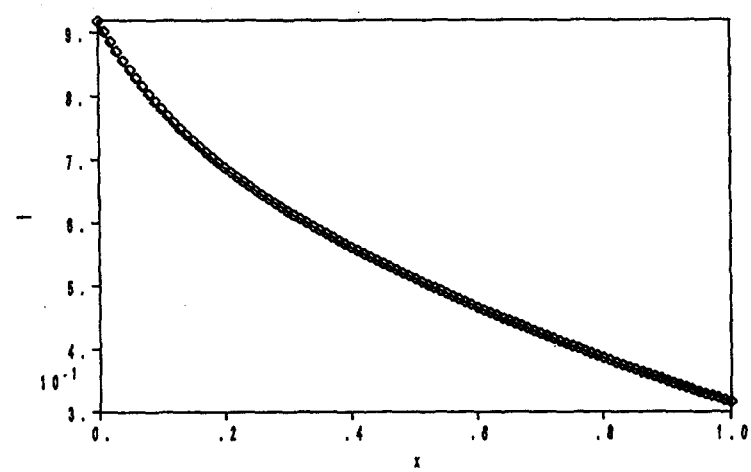

Figure A7. The exact and CMQ plots of the FRAC function.

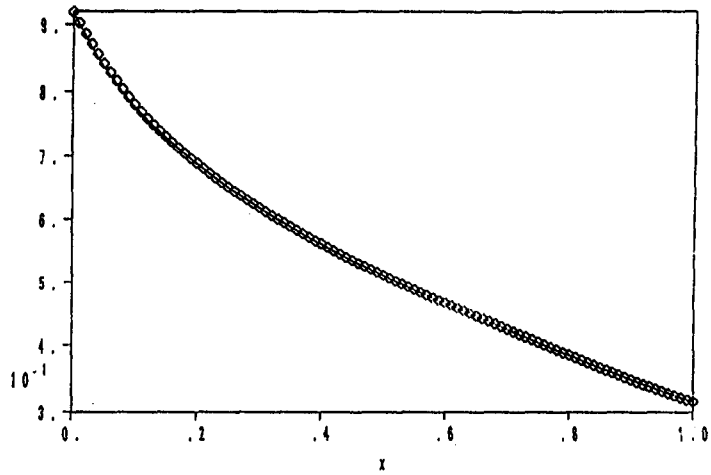

Figure A8. The exact and VMQ plots of the FRAC function.

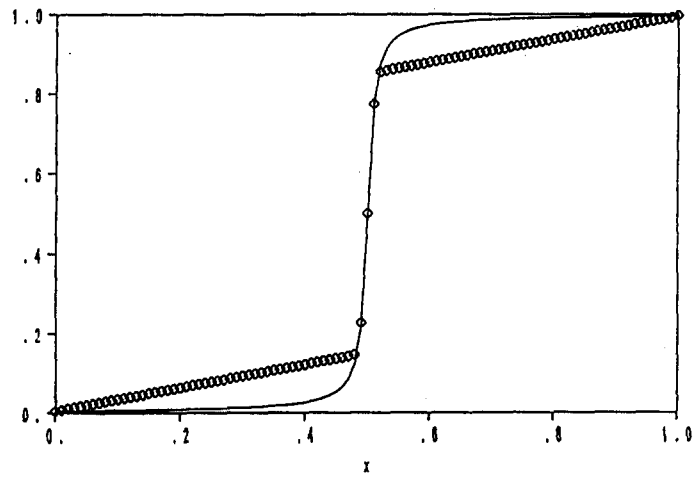

Figure A9. The exact and CMQ plots of the STEP function.

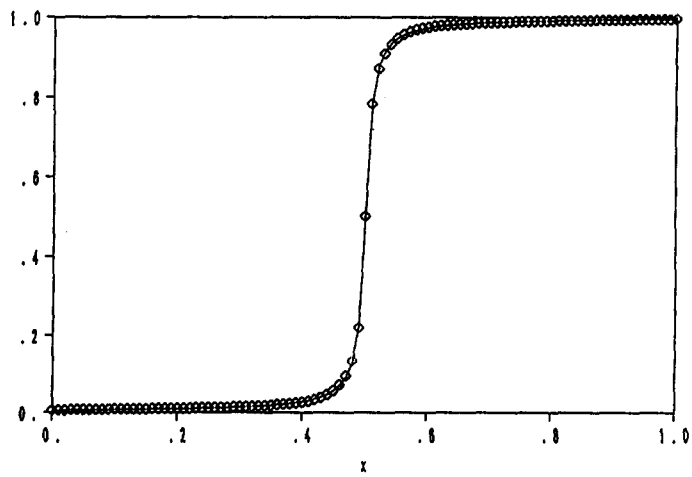

Figure A10. The exact and VMQ plots of the STEP function.

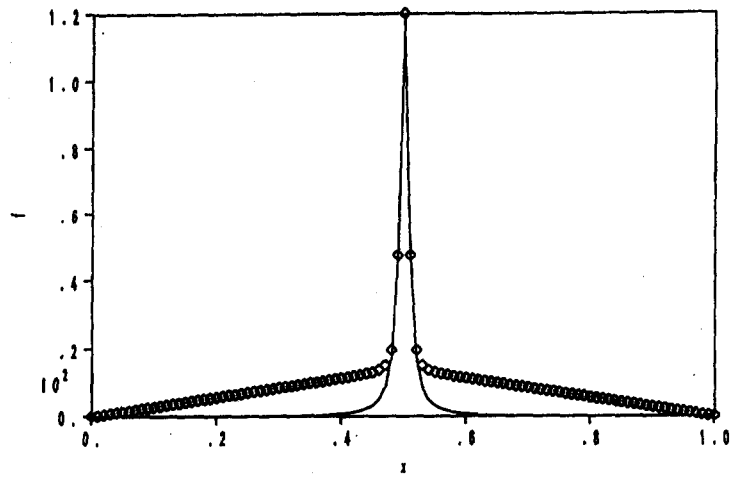

Figure A11. The exact and CMQ plots of the DELTA function.

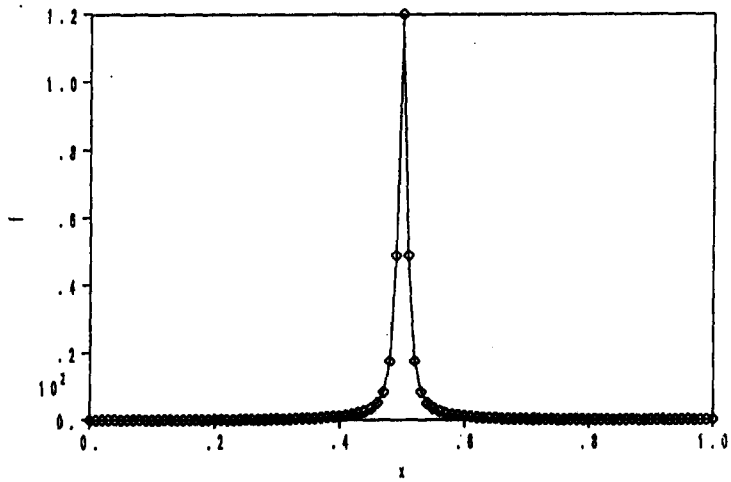

Figure A12. The exact and VMQ plots of the DELTA function.

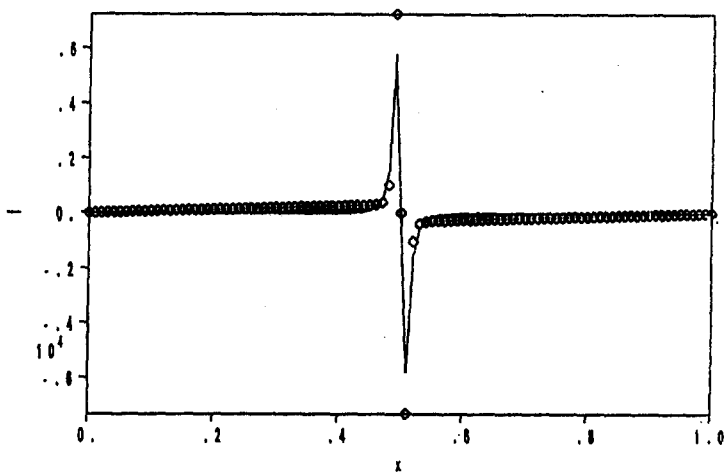

Figure A13. The exact and CMQ plots of the DDLT function.

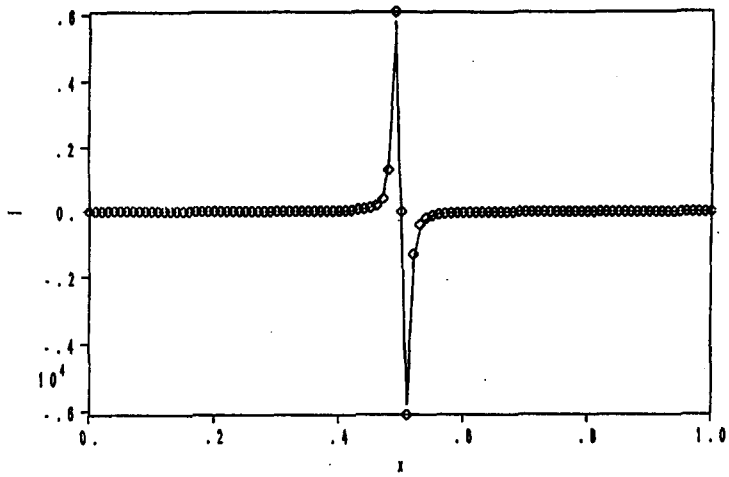

Figure A14. The exact and VMQ plots of the DDLT function.

APPENDIX B

PLOTS OF THE FRANKE 25 POINT DATA SET, EXACT FUNCTIONS AND SELECTED RMQ INTERPOLANTS

In the table below, we present the variable R^2, MQ scheme, and exact plots of each of the six Franke functions. Figure B1 is the bivariate 25 point data set of Franke used for each of the six Franke test functions.

Table B1. Summary of list of figures for the Franke functions, with plots of results for VMQ, and exact function.

FUNCTION NUMBER	Exact Function	VMQ Variable R^2
1	Figure B2	Figure B3
2	Figure B4	Figure B5
3	Figure B6	Figure B7
4	Figure B8	Figure B9
5	Figure B10	Figure B11
6	Figure B12	Figure B13

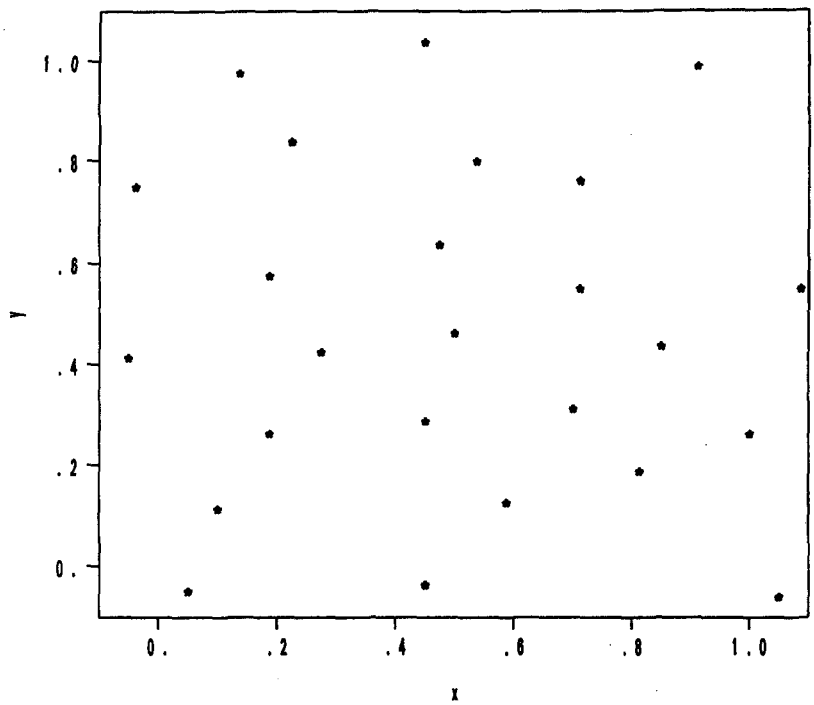

Figure B1. The bivariate 25 point data set of Franke.

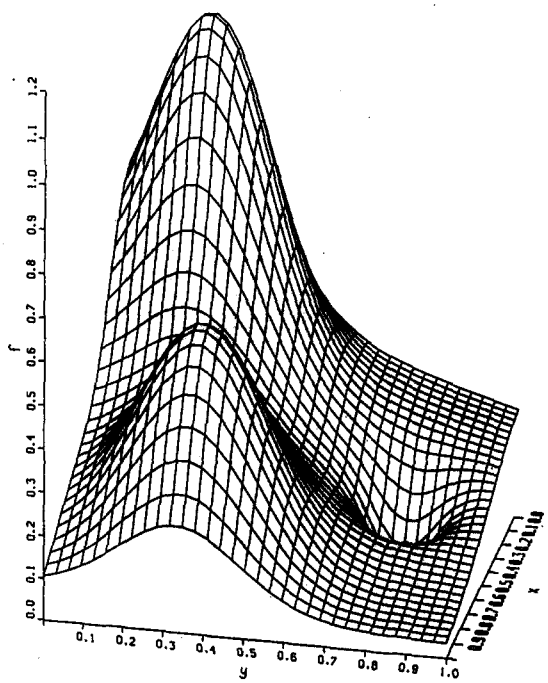

Figure B2. The exact plot of Franke's function 1.

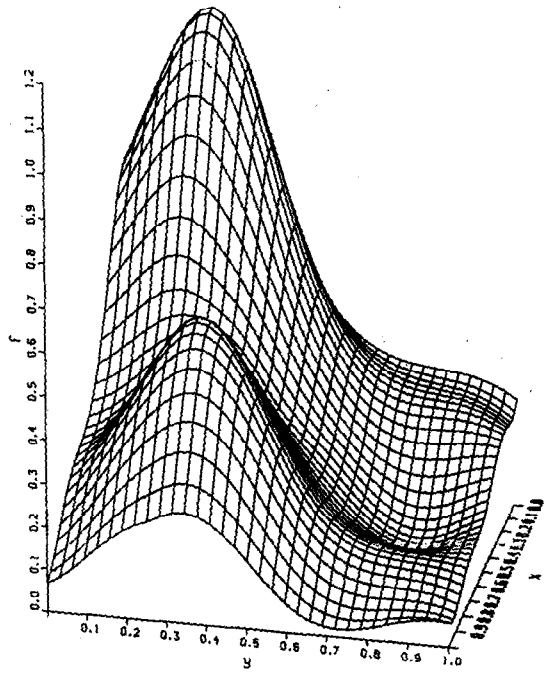

Figure B3. The best VMQ plot of Franke's function 1.

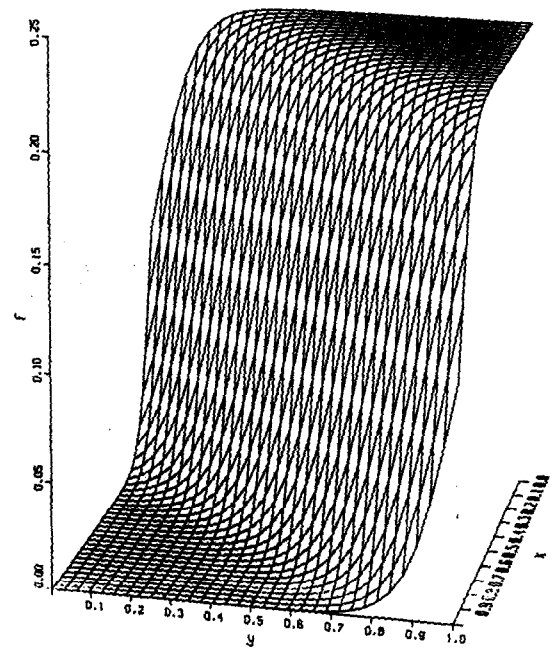

Figure B4. The exact plot of Franke's function 2.

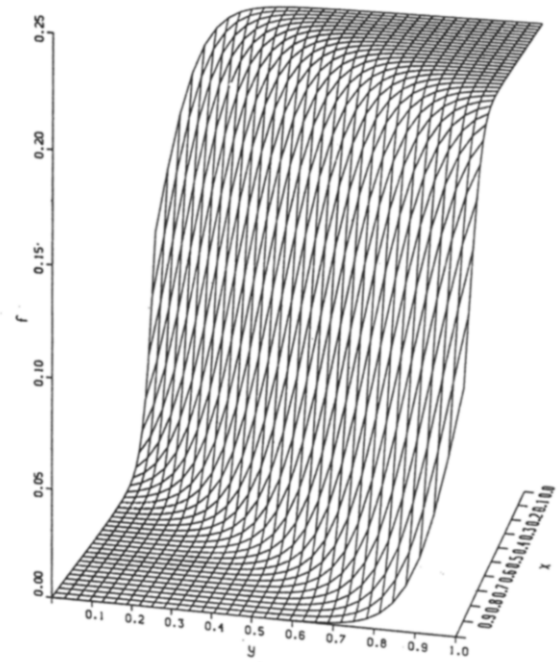

Figure B5. The best VMQ plot of Franke's function 2.

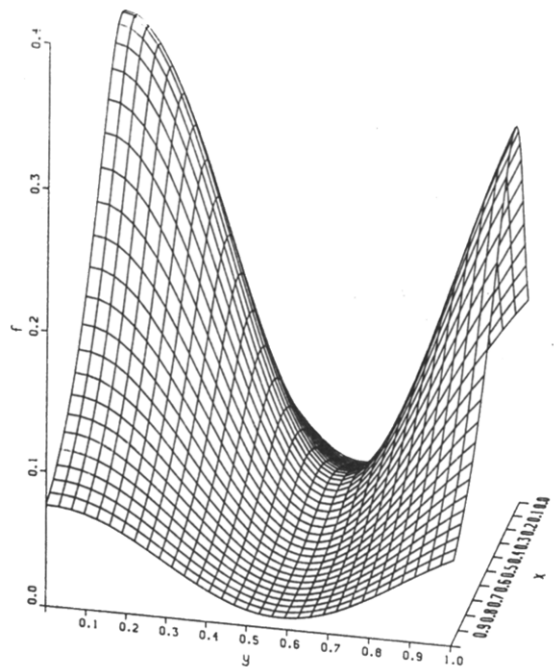

Figure B6. The exact plot of Franke's function 3.

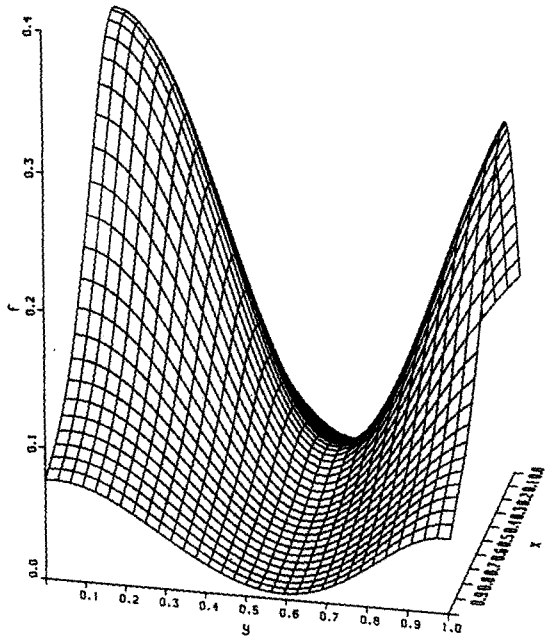

Figure B7. The best VMQ plot of Franke's function 3.

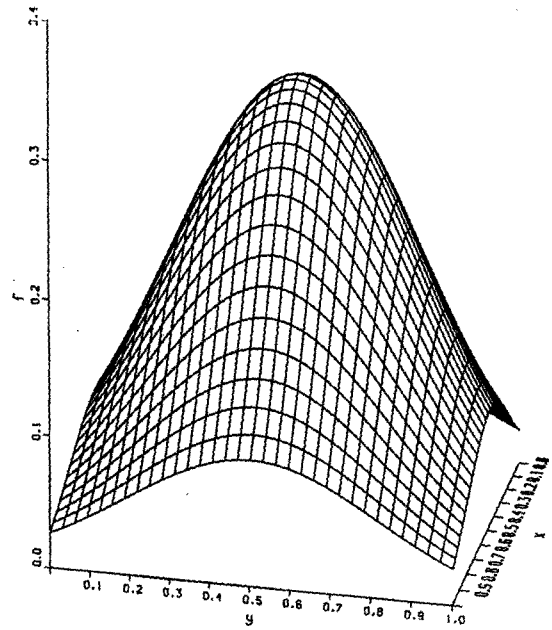

Figure B8. The exact plot of Franke's function 4.

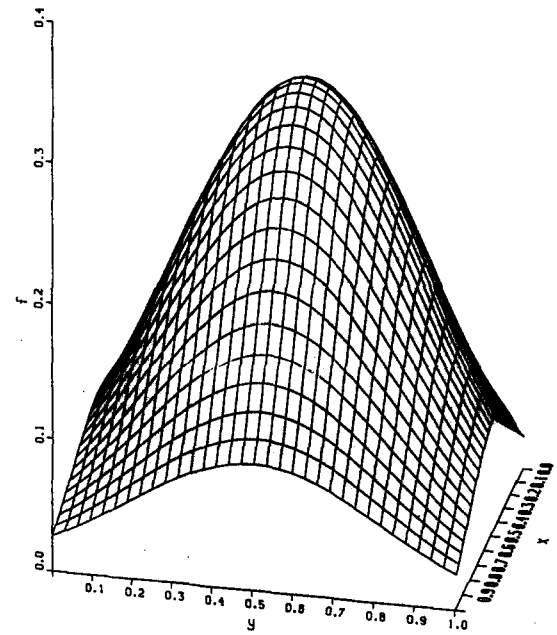

Figure B9. The best VMQ plot of Franke's function 4.

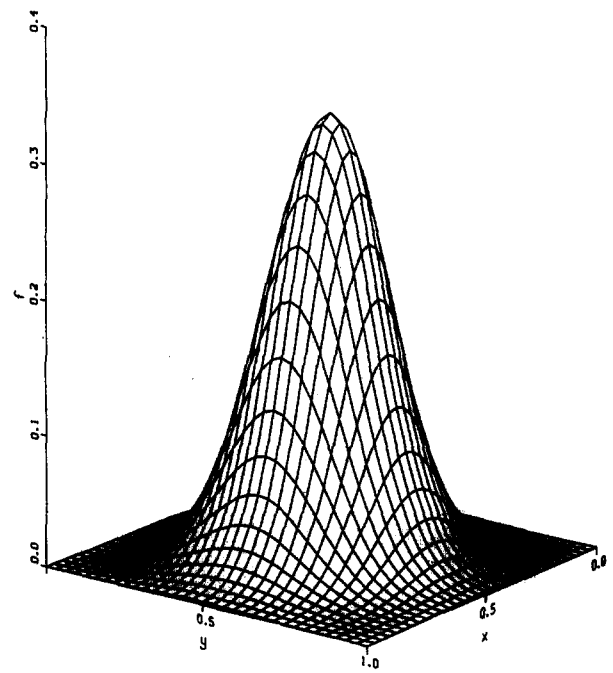

Figure B10. The exact plot of Franke's function 5.

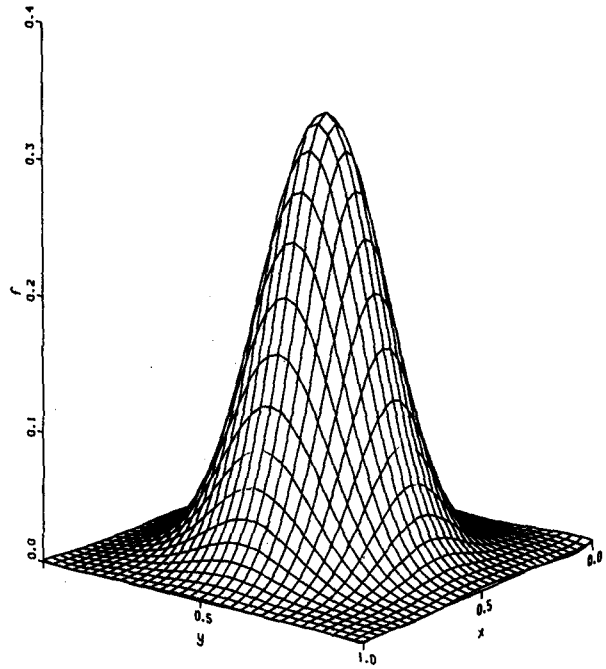

Figure B11. The best VMQ plot of Franke's function 5.

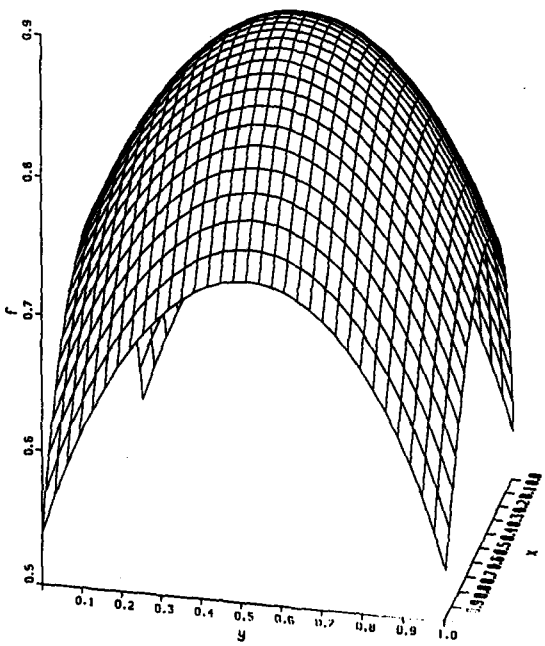

Figure B12. The exact plot of Franke's function 6.

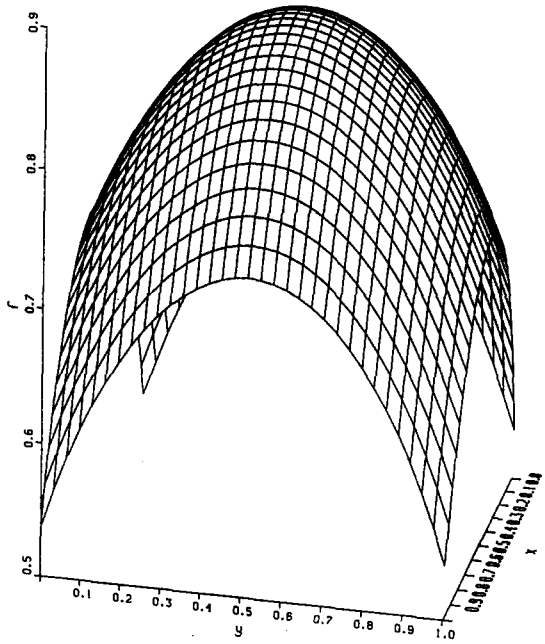

Figure B13. The best VMQ plot of Franke's function 6.